



Synthesis, radiofluorination and pharmacological evaluation of a fluoromethyl spirocyclic PET tracer for central σ_1 receptors and comparison with fluoroalkyl homologs

Aurélie Maisonia^{b,1}, Eva Große Maestrup^{a,1}, Christian Wiese^a, Achim Hiller^b, Dirk Schepmann^a, Steffen Fischer^b, Winnie Deuther-Conrad^b, Jörg Steinbach^b, Peter Brust^b, Bernhard Wünsch^{a,*}

^aInstitut für Pharmazeutische und Medizinische Chemie der Universität Münster, Hittorfstraße 58-62, D-48149 Münster, Germany

^bHelmholtz-Zentrum Dresden-Rossendorf, Research Site Leipzig, Institute of Radiopharmacy, Division of Neuroradiopharmaceuticals, Permoserstraße-15, D-04318 Leipzig, Germany

ARTICLE INFO

Article history:

Received 20 September 2011

Revised 31 October 2011

Accepted 2 November 2011

Available online 9 November 2011

Keywords:

σ_1 Receptor radioligands

Spirocyclic piperidines

Fluorine-18

Neuroimaging

Structure–affinity relationship

Fluoroalkyl homologs

ABSTRACT

The spirocyclic σ_1 receptor ligand **1** (1'-benzyl-3-(fluoromethyl)-3H-spiro[[2]benzofuran-1,4'-piperidine]) was prepared in four steps starting from methoxy derivative **5**. Due to its high σ_1 affinity ($K_i = 0.74$ nM) and selectivity against several other relevant targets, **1** was investigated as ¹⁸F-labeled PET tracer and its biological properties were compared with those of homologous fluoroalkyl derivatives **2–4**. The fluoromethyl derivative **1** was faster metabolized in vitro than homologs **2–4**. In contrast to the radiosynthesis of [¹⁸F]**2–4**, the nucleophilic substitution of the tosylate **15** using the K[¹⁸F]F–K₂₂₂-carbonate complex required heating to 150 °C in DMSO to achieve high labeling efficiencies. Whereas radiometabolites of [¹⁸F]**2–4** were not detected in vivo in the brain of mice, two radiometabolites of [¹⁸F]**1** were found. Analysis of ex vivo autoradiography images provided rather low target-to-nontarget ratio for [¹⁸F]**1** compared with [¹⁸F]**2–4**. [¹⁸F]**1** showed a fast uptake in the brain, which decreased continuously over time. The brain-to-plasma ratio of the radiotracer [¹⁸F]**1** was only exceeded by the fluoroethyl tracer [¹⁸F]**2**.

© 2011 Elsevier Ltd. All rights reserved.

1. Introduction

The sigma (σ) receptor was first discovered about 30 years ago as a new subtype of opioid receptors.¹ At present it is known that σ receptors possess specific drug selectivity patterns, differential anatomical distribution, and unique properties which are different from opioid and other known neurotransmitter and hormone receptor families. Pharmacological data based on binding studies, anatomical distribution, and biochemical features distinguish at least two σ receptor subtypes (σ_1 and σ_2) which have recently been characterized.^{2–6} The human σ_1 receptor is a unique protein consisting of 223 amino acids, which was first cloned and functionally expressed by Kekuda et al.⁷

The σ_1 receptor has long been considered to be an orphan receptor. Recently, Fontanilla et al.⁸ have demonstrated that the naturally

occurring hallucinogen *N,N*-dimethyltryptamine (DMT) is an endogenous ligand for σ_1 receptors. Unlike the classical plasma-membrane bound neurotransmitter receptors the σ_1 receptor resides specifically at the endoplasmic reticulum (ER)-mitochondrion interface called the mitochondrion-associated ER membrane (MAM).⁹ It is a ligand-activated molecular chaperone that assists the folding or unfolding and the assembly or disassembly of other macromolecular structures and is proposed to act as inter-organelle signaling modulator. The σ_1 receptor ligands, including DMT, at concentrations close to their K_i values, are suggested to cause the dissociation of σ_1 receptors from another ER chaperone, binding immunoglobulin protein (BiP), allowing σ_1 receptors to chaperone inositol 1,4,5-trisphosphate receptors (IP3Rs) at the MAM. Higher concentrations of DMT are assumed to cause the translocation of σ_1 receptors from the MAM to the plasma membrane, leading to the inhibition of voltage-gated ion channels.⁹ Thus, σ_1 receptor ligands might shift the site of action of σ_1 receptor chaperones from the center of the cell to its periphery. In good agreement with this model is a recent finding obtained using σ_1 receptor knockout mice which identified the σ_1 receptor as a part of mechanisms modulating activity-induced sensitization in pain pathways.¹⁰ This and other related findings provide evidence to consider selective σ_1 receptor antagonists an innovative and alternative approach for treating neuropathic pain.¹¹

Abbreviations: DMT, *N,N*-dimethyltryptamine; MAM, mitochondrion-associated ER membrane; ER, endoplasmic reticulum; BiP, binding immunoglobulin protein; IP3R, inositol 1,4,5-trisphosphate receptor; PET, positron emission tomography; EMP, emopamil-binding protein; VAcHT, vesicular acetylcholine transporter; p.i., post injection; ID, injected dose.

* Corresponding author. Tel.: +49 251 8333311; fax: +49 251 8332144.

E-mail address: wuensch@uni-muenster.de (B. Wünsch).

¹ These authors contributed equally to this work.

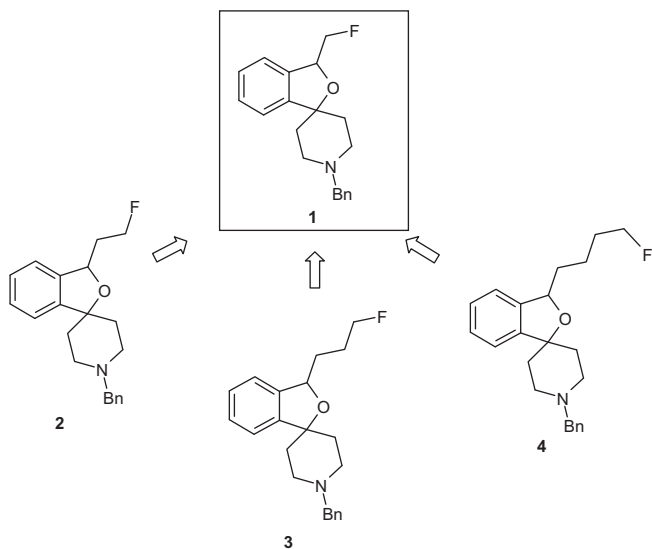


Figure 1. Spirocyclic σ_1 ligands with different (fluoroalkyl) residues in 3-position.

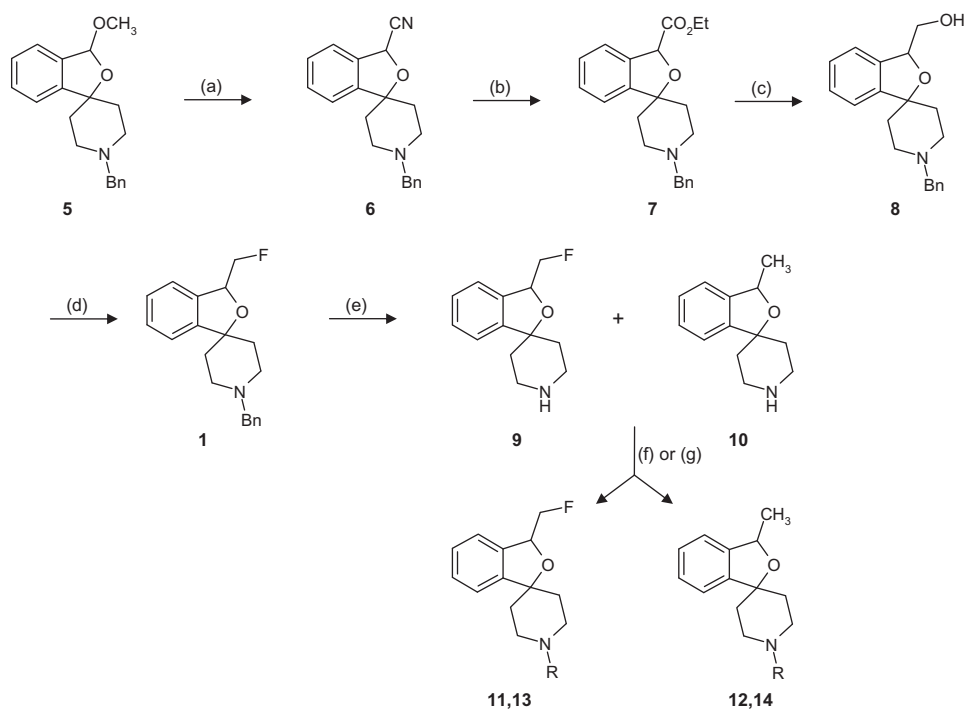
Related to the concept described above is also the recent discovery of heteromers consisting of σ_1 receptors and dopamine D_1 receptors which provides a molecular explanation for D_1 receptor-mediated behavioral effects of cocaine.¹² Beside drug addiction there is strong evidence that σ_1 receptors play a major role in the pathophysiology of depression. Behavioral models revealed that ligands which bind to σ_1 receptors possess antidepressant-like properties with fast onset of action.^{13,14} This is further supported by a recent gene-based association analysis between σ_1 receptor gene expression and major depressive disorder in the Japanese population,¹⁵ the development of a depressive-like phenotype in σ_1 receptor knockout mice¹⁶ and the consideration of σ_1 receptor-mediated antidepressive effects of fluvoxamine.^{17,18} Interestingly,

fluvoxamine has also been reported to dramatically decrease delirium rating scale scores of patients in intensive care units¹⁹ and it has been hypothesized that selective serotonin reuptake inhibitors such as fluvoxamine may reduce the risk of transition of people with prodromal symptoms to schizophrenia.²⁰ Accordingly, σ_1 receptors are considered as novel therapeutic targets for the pharmacotherapy of depression, anxiety and various other brain diseases.^{21–25} Related to this development it has been reviewed that σ_1 receptor imaging is useful for studying the pathophysiology of neurological and psychiatric disorders and for evaluation of the pharmacodynamics of psychiatric drugs.²⁶

The only PET radioligand that was used for neuroimaging of σ_1 receptors in humans so far is [¹¹C]SA4503. Studies were performed in patients with Parkinson's disease²⁷ and Alzheimer's disease.²⁸ Recently some methodical aspects were in the main focus of the human studies. Thus, combination with blood flow measurement, a shortened protocol for the receptor quantification and improvement in parametric imaging were proposed.^{29–31} Notably, [¹¹C]SA4503 has high affinity not only to σ_1 receptors (K_i values in the range of 4–14 nM^{32–34}) but also to other targets such as the vesicular acetylcholine transporter (VACHT, $K_i = 50$ nM³⁴) and the emopamil binding protein (EBP, $K_i = 1.7$ nM³⁵) which may be of high impact for the interpretation of neuroimaging findings.

A few years ago, we focused our research on the development of alternative fluorinated σ_1 receptor ligands, which could be used for noninvasive in vivo PET imaging of central σ_1 receptors. These studies led to an innovative compound class of spirocyclic piperidines. In particular, ligands with a spiro[benzofuran-piperidine] scaffold met two important requirements for a radiotracer by combining very high affinity with suitable selectivity to σ_1 receptors.^{36–43} Therefore, this scaffold was used as a very promising starting point for further structural modifications to develop a fluorinated PET tracer for imaging of σ_1 receptors in the central nervous system.

We have synthesized three new spirocyclic piperidines **2–4** (Fig. 1) bearing fluoroalkyl residues with different chain lengths ($n = 2–4$) in position 3.^{43–47} These fluoroalkyl derivatives **2–4**



Scheme 1. Synthesis of spirocyclic σ_1 receptor ligands with a (fluoromethyl) residue in 3-position. Reagents and conditions: (a) Me_3SiCN , $\text{BF}_3 \cdot \text{OEt}_2$, CH_2Cl_2 , 20 min, -25 °C, 1 h, $3–5$ °C, 87%. (b) H_2SO_4 , EtOH, 19 h, reflux, 57%. (c) LiAlH_4 , THF, 30 min, -20 °C, 72%. (d) Et_2NSF_3 (DAST), CH_2Cl_2 , 30 min, -78 °C, 19 h, rt, 70%. (e) NH_4HCO_2 , Pd/C, CH_3OH , 3 h, reflux, 92% (**9–10**). (f) $\text{FC}_6\text{H}_4\text{CH}_2\text{Cl}$, CH_3CN , K_2CO_3 , 8 h, reflux, 23% (**11**), 10% (**12**). (g) $\text{PhCH}(\text{CH}_3)\text{Br}$, CH_3CN , K_2CO_3 , 8 h, reflux, 8% (**13**), 11% (**14**).

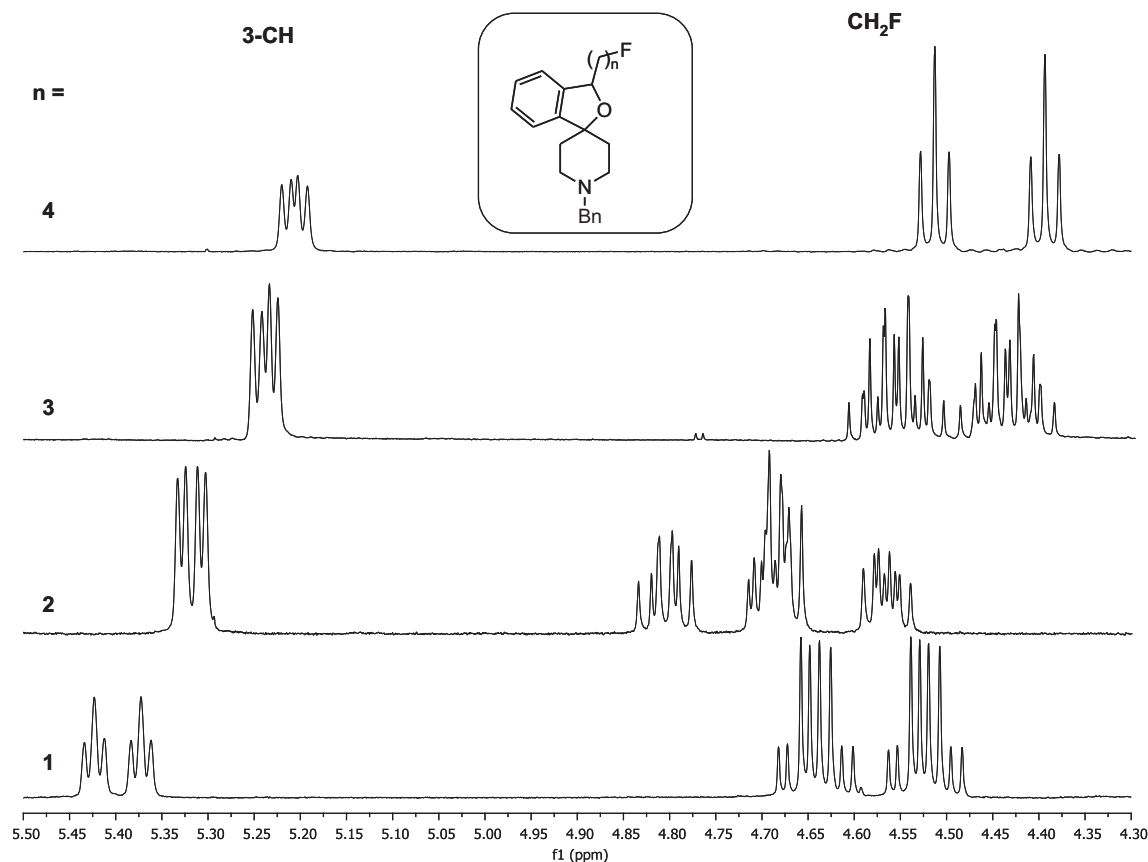
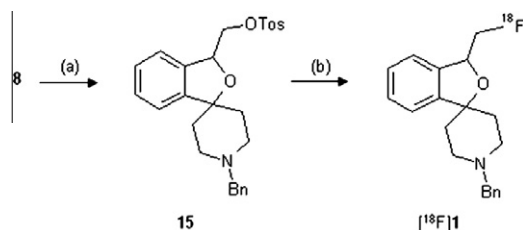


Figure 2. Comparison of characteristic ^1H NMR signals of the four homologous (fluoroalkyl) σ_1 ligands **1–4**: **1**: 5.40 ppm (dt, 3-CH), 4.56 ppm (ddd, CH_2F), 4.61 ppm (ddd, CH_2F), $J(\text{H}-\text{C}-\text{F}) = 47.3$ Hz. **2**: 5.32 ppm (dd, 3-CH), 4.63 ppm (dddd, CH_2F), 4.75 ppm (dddd, CH_2F), $J(\text{H}-\text{C}-\text{F}) = 46.9$ Hz. **3**: 5.24 ppm (dd, 3-CH), 4.49 ppm (ddt, CH_2F), 4.53 ppm (dddd, CH_2F), $J(\text{H}-\text{C}-\text{F}) = 47.2$ Hz. **4**: 5.21 ppm (dd, 3-CH), 4.46 ppm (dt, 2 H, CH_2F), $J(\text{H}-\text{C}-\text{F}) = 47.3$ Hz.



Scheme 2. Synthesis of precursor **15** and radiosynthesis of $[^{18}\text{F}]\mathbf{1}$. Reagents and conditions: (a) TosCl, DMAP, NEt_3 , CH_2Cl_2 , -25 °C, 30 min, then rt, 21 h, 88%. (b) $\text{K}[^{18}\text{F}]\text{F}-\text{K}_{222}$ -carbonate complex, DMF, 150 °C, 20 min, 72–86%.

possess very high σ_1 receptor affinity ($K_i = 0.59$ – 1.4 nM, see Table 1) and high selectivity over the σ_2 subtype (422- to 1331-fold). These homologs differed in polarity, penetration into the central nervous system and biotransformation during in vivo experiments. These results prompted the biological characterization of the smallest member of this homologous series, the fluoromethyl derivative **1** (Fig. 1). Herein, we report on the synthesis as well as radiosynthesis and the biological evaluation of the new ligand **1**. Additionally, the chemical, physical and biological properties of all the four homologous fluoroalkyl derivatives **1–4** will be comparatively discussed.

2. Results and discussion

2.1. Synthesis

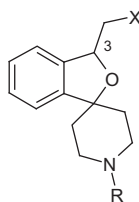
The synthesis of the fluoromethyl substituted piperidine **1** is depicted in Scheme 1 and started with the methoxy derivative **5**.³⁹

The acetalic methoxy group of **5** was replaced with a cyano group upon treatment with trimethylsilyl cyanide (Me_3SiCN) and boron trifluoride diethyl ether complex ($\text{BF}_3 \cdot \text{OEt}_2$). The resulting nitrile **6** was converted into the ester **7** using ethanol and concentrated sulfuric acid.³⁸ Primary alcohol **8** was produced by reduction of **7** with lithium aluminum hydride (LiAlH_4). Reaction of the primary alcohol **8** with diethylaminosulfur trifluoride (DAST) provided the fluorinated derivative **1** in 70% yield.

Since important metabolic pathways of this compound class are hydroxylation in position 4 of the *N*-benzyl residue and *N*-debenzylation,^{36,42,43,45,47} we decided to investigate the corresponding *p*-fluorobenzyl and 1-phenylethyl derivatives **11** and **13**, which should be metabolically more stable. In order to modify the residue at the piperidine *N*-atom, the *N*-benzyl group of **1** was removed hydrogenolytically with ammonium formate in the presence of Pd/C.⁴⁸ Purification by flash chromatography led to 92% of a mixture, containing the desired fluoromethyl derivative **9** together with the methyl derivative **10** (ratio **9**:**10** = 69:31). In addition to the *N*-benzyl residue, the fluorine atom was cleaved off reductively during the very mild transfer hydrogenolysis. An analogous reductive defluorination had not been observed for homologs **2–4** bearing a 2-fluoroethyl,⁴⁴ 3-fluoropropyl,⁴⁵ or 4-fluorobutyl⁴⁶ residue in position 3, respectively. The unexpected defluorination of **1** may originate from the β -fluoroether substructure, which is unique among these four fluoroalkyl derivatives. The formation of an oxiranium ion as reactive intermediate is postulated.

The mixture of fluoromethyl derivative **9** and methyl compound **10** was alkylated either with *p*-fluorobenzyl chloride or 1-bromo-1-phenylethane to afford corresponding tertiary amines **11/12** and **13/14**, which were separated by flash chromatography, respectively.

Table 1
 σ_1 and σ_2 receptor affinities of spirocyclic piperidines with substituted alkyl residues in 3-position



Compd	R	X	$K_i \pm \text{SEM}$ [nM] ($n = 3$)		σ_1/σ_2 Selectivity
			σ_1	σ_2	
1	C ₆ H ₅ CH ₂	F	0.74 ± 0.34	550	743
2	C ₆ H ₅ CH ₂	CH ₂ F	0.59 ± 0.20	785	1331
3	C ₆ H ₅ CH ₂	(CH ₂) ₂ F	1.4 ± 0.26	837	620
4	C ₆ H ₅ CH ₂	(CH ₂) ₃ F	1.2 ± 0.46	489	422
8	C ₆ H ₅ CH ₂	OH	4.5 ± 2.5	IC ₅₀ >1 μM	>220
11	FC ₆ H ₄ CH ₂	F	0.14 ± 0.08	89 ± 9	636
12	FC ₆ H ₄ CH ₂	H	1.1 ± 0.31	925	841
13	C ₆ H ₅ CH(CH ₃)	F	3.6 ± 0.63	IC ₅₀ >1 μM	>275
14	C ₆ H ₅ CH(CH ₃)	H	9.2 ± 4.8	824	90
15	C ₆ H ₅ CH ₂	OTos	2.9 ± 0.08	IC ₅₀ >1 μM	>345
Haloperidol			6.3 ± 1.6	78 ± 2.3	12
(+)-Pentazocine			5.7 ± 2.2	–	–

¹H NMR signals characteristic of the four homologous fluoroalkyl derivatives **1–4** are compared in Figure 2. With increasing distance between the proton in position 3 of the 2-benzofuran ring and the electronegative fluorine atom, the chemical shift of this signal is decreasing continuously (**1**: $\delta = 5.40$ ppm, **4**: $\delta = 5.21$ ppm, Fig. 2). Interestingly, for the derivatives **2–4** doublets of doublets are observed for this proton, whilst in the shortest (fluoromethyl) derivative **1** an H–F-coupling over three bonds with a coupling constant of 20.4 Hz renders this signal a doublet of triplets. The signals of the CH₂F groups are characterized by a very large H–F-coupling (J ca. 47 Hz) over two bonds. Whereas the CH₂F protons of the (4-fluorobutyl) derivative **4** are magnetically equivalent (long distance to the stereogenic center) these protons are magnetically different in the shorter homologs **1–3**, which leads to ddd (**1**), dddd (**2**), or ddt (**3**) fine structures of the signals.

The tosylate precursor **15** chosen as starting material for radiolabeling was synthesized from the alcohol **8**, which was converted into the tosylate **15** upon reaction with tosyl chloride in the presence of triethylamine and 4-(dimethylamino)pyridine (see Scheme 2).

2.2. Receptor affinity

Competition experiments with radioligands were used for determining σ receptor affinities of the spirocyclic compounds. In the σ_1 assay homogenates of guinea pig brains were used as receptor material and the σ_1 selective ligand [³H]-(+)-pentazocine was employed as radioligand. Rat liver homogenates served as source for σ_2 receptors in the σ_2 assay. Since a σ_2 selective radioligand is not commercially available, the nonselective radioligand [³H]-1,3-di(*o*-tolyl)guanidine was employed in the presence of an excess of nontritiated (+)-pentazocine, which selectively masks σ_1 receptors.^{49,50}

The σ_1 and σ_2 receptor affinities of the fluorinated and methylated spirocyclic piperidines are summarized in Table 1. The σ_1 receptor affinity of the fluoromethyl derivative **1** ($K_i = 0.74$ nM) is in the same range as the σ_1 affinity of the homologous fluoroalkyl derivatives **2–4**.^{44–47} The σ_2 receptor affinity test performed with **1** ($K_i = 550$ nM) resulted in an excellent σ_1/σ_2 selectivity (factor

743). Altogether, the σ_1 receptor affinity and σ_1/σ_2 selectivity of the four homologous fluoroalkyl derivatives **1–4** are comparable.

In addition to the fluoromethyl derivative **1**, the σ receptor affinities of the alcohol **8** and the tosylate precursor **15** were recorded. Compared with **1** the σ_1 affinity of the polar alcohol **8** is sixfold reduced. However, compound **15** showed a rather high σ_1 affinity ($K_i = 2.9$ nM), which will be exploited together with the strong alkylating activity of **15** for the development of a σ_1 ligand, which can be covalently bound to the σ_1 receptor protein.

While the introduction of a fluorine atom in *p*-position of the *N*-benzyl residue (**11**) led to fivefold increase of the σ_1 receptor affinity, the introduction of a methyl group in α -position of the *N*-benzyl residue (**13**) resulted in a fivefold decrease of σ_1 affinity. However, the very potent *p*-fluorobenzyl derivative **11** revealed a rather high σ_2 affinity ($K_i = 89$ nM). Although the σ_1/σ_2 selectivity is still acceptable, the *p*-fluorobenzyl derivative **11** was not considered for further development.

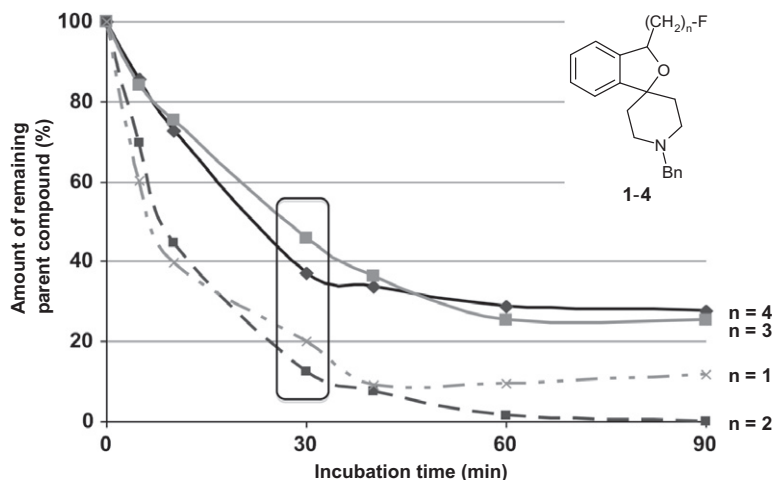
Replacement of the fluorine atom with a proton resulted in a 3- to 10-fold reduced σ_1 receptor affinity of the methylated compounds **12** and **14**. Obviously, the fluorine atom at the methyl residue in position 3 is favorable for high σ_1 receptor affinity.

In addition to the interactions with σ_1 and σ_2 receptors, the affinities of the fluoroalkyl derivatives **1–4** towards related receptors and proteins were investigated. Since potent NMDA and σ receptor ligands are often very similar, the NMDA receptor affinity was taken into account. Originally, the σ receptor has been classified as opioid receptor subtype. Therefore, the affinities towards μ , κ , and δ opioid receptors were determined. The interactions of the fluoroalkyl derivatives **2–4** with the vesicular acetylcholine transporter (VACHT) and the emopamil-binding protein (EBP), which is a vertebrate sterol isomerase, were also recorded, since some potent σ_1 ligands (e.g., SA4503) possess considerable affinity towards these target systems.

The results of these receptor binding studies are given in Table 2. At a test compound concentration of 1 μM the binding of the radioligand [³H]MK-801 towards the phencyclidine binding site was not reduced. However, moderate affinities of the fluoroalkyl derivatives **1–4** towards the opioid receptors were observed. The rather

Table 2Receptor selectivity: affinity of the four homologous fluoroalkyl derivatives **1–4** towards related receptors and proteins

Compd	K_i [nM] ($n = 3$)							
	σ_1	σ_2	NMDA (μM)	μ	κ	δ	VACHT (μM)	EBP
1	0.74	550	>1	481	918	152	—	—
2	0.59	785	>1	456	372	>1 μM	1.4	211
3	1.4	837	>1	246	368	209	>1	455
4	1.2	489	>1	605	419	>1 μM	>1	233

**Figure 3.** Comparison of the rate of biotransformation of the four fluoroalkyl derivatives **1–4**. With exception of the curve of the 3-fluoropropyl compound **3** all data points were recorded twice.

high δ -opioid receptor affinity of the fluoromethyl (**1**, $K_i = 152$ nM) and 3-fluoropropyl derivative **3** ($K_i = 209$ nM) are noteworthy. Nevertheless, the σ_1/δ -selectivity is still high (205 for **1**, 150 for **3**). Among this series of compounds, the 2-fluoroethyl derivative **2** with the highest σ_1 affinity shows the best selectivity against all three opioid receptors (763 (σ_1/μ), 630 (σ_1/κ), >1000 (σ_1/δ)). The affinities of the fluoroalkyl derivatives **2–4** towards the VACHT as well as the EBP were very low, indicating high selectivity against these related proteins.

2.3. In vitro rate of degradation with rat liver microsomes

Since the fluoromethyl derivative **1** was promising for further studies in vivo, its rate of degradation upon incubation with rat liver microsomes was investigated. In Figure 3, the concentration of parent compound **1** after definite time intervals is compared with the concentration of homologous compounds **2–4**.

For the investigation of the metabolic degradation six incubations were started at the same time and stopped after definite time intervals to observe the decomposition. Directly after termination of the metabolic process, the internal standard praziquantel was added to quantify the remaining parent compounds by HPLC analyses. A matrix calibration was carried out for all spirocyclic σ_1 ligands.

The rate of metabolic degradation in vitro correlates with the length of the fluoroalkyl residue in position 3. Whereas compounds **1** and **2** with short fluoroalkyl side chains were biotransformed very fast, the metabolic degradation of the corresponding homologs **3** and **4** was considerably slower. After an incubation period of 30 min, approximately 20% of compound **1** and 13% of compound **2** remained unchanged, but 38% and 45% of the derivatives **3** and **4**, respectively, were detected by HPLC analyses. Therefore, regarding the rate of in vitro metabolic degradation longer fluoroalkyl residues seem to be favored over shorter ones.

2.4. Radiosynthesis

The radiosynthesis of the radiotracer [^{18}F]**1** from the tosylate **15** (Scheme 2) was more difficult and differed from the syntheses of the three other radiotracers [^{18}F]**2–4** of the fluoroalkyl series studied. Indeed, reaction of the precursor **15** with [^{18}F]fluoride in acetonitrile at 83 °C according to the reaction parameters previously optimized for [^{18}F]**4** led to a labeling efficiency always below 16% (Fig. 4A). This result is in sharp contrast to the data obtained with the homologous fluoroalkyl derivatives [^{18}F]**2–4**, which were produced with this method in very high labeling yields. To circumvent this problem, other solvents such as *N,N*-dimethylformamide (DMF) and dimethylsulfoxide (DMSO) allowing higher reaction temperatures were investigated. With a constant precursor concentration of 2 mg/mL the best labeling efficiencies were obtained with DMSO at 150 °C (57% after 10 min) (Fig. 4A). A few microwave-assisted labeling experiments were conducted in DMF (~75 W, up to 130 °C) which also resulted in good labeling efficiencies (~60%) but were less reproducible than the conventional heating protocol.

Further modifications of the concentration of the precursor resulted in optimized conditions with 2.5–3 mg/mL of tosylate **15** in DMSO under conventional heating (150 °C, Fig. 4B) providing labeling efficiencies of 65–70% after a reaction time of 10–15 min. The crude product was then purified by isocratic semipreparative RP-HPLC, followed by solid phase extraction. The radiotracer [^{18}F]**1** was finally produced with radiochemical yields of 38–50%, radiochemical purities >99.1%, and high specific activities of 173–412 GBq/ μmol ($n = 6$).

2.5. In vitro stability and lipophilicity

Next the in vitro stability of [^{18}F]**1** was investigated under physiological conditions. The amount (in %) of the unchanged radiotracer after an incubation period of 2 h at 40 °C in 0.9% sodium

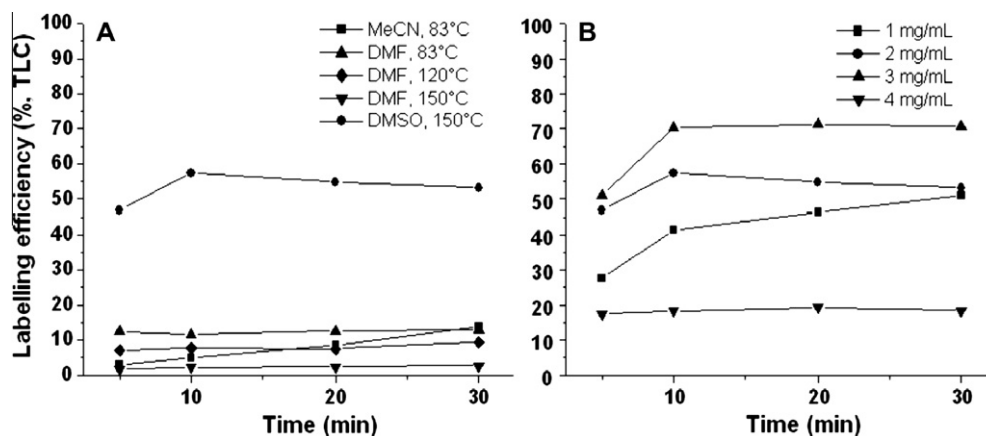


Figure 4. Labeling efficiency of $[^{18}\text{F}]\mathbf{1}$ using different solvents and temperatures (A) and different precursor concentrations (B).

Table 3

In vitro stability of $\mathbf{1-4}$ after an incubation period of 2 h in different buffer systems ($n = 2$)

	$[^{18}\text{F}]\mathbf{1}$ (%)	$[^{18}\text{F}]\mathbf{2}$ (%)	$[^{18}\text{F}]\mathbf{3}$ (%)	$[^{18}\text{F}]\mathbf{4}$ (%)
0.9% NaCl solution, pH 7.2, 40 °C	96.9	97.1	>99	97.9
Phosphate-saline-solution, pH 7.2, 40 °C	96.5	98.4	98.0	94.7
0.01 M TRIS-HCl, pH 7.4, 21 °C	100	97.6	>98	95.4

Table 4

Log D values of the spirocyclic piperidines $\mathbf{1-4}$ ($n = 3$)

	ACD/log D software pH 7.2	<i>n</i> -Octanol/phosphate buffer pH 7.2	<i>n</i> -Octanol/phosphate-saline-solution pH 7.2
Log D $[^{18}\text{F}]\mathbf{1}$	2.83	2.45 ± 0.04	2.39 ± 0.04
Log D $[^{18}\text{F}]\mathbf{2}$	3.10	2.70 ± 0.32	2.57 ± 0.32
Log D $[^{18}\text{F}]\mathbf{3}$	3.47	3.00 ± 0.05	2.78 ± 0.06
Log D $[^{18}\text{F}]\mathbf{4}$	3.83	3.16 ± 0.11	3.11 ± 0.14

chloride solution (pH 7.2), phosphate-saline-solution (pH 7.2) or 0.01 M TRIS-HCl buffer (pH 7.4 at 21 °C) are summarized in Table 3 and compared with values previously determined for $[^{18}\text{F}]\mathbf{2-4}$. According to radio-TLC and analytical radio-HPLC measurements, the four radiotracers showed an excellent to sufficient stability under the conditions tested. In particular, defluorination of the radioligands was not observed.

The estimation of the lipophilicity of radiotracers developed for neuroimaging is an important tool in predicting their blood-brain-barrier permeability. In this study, log D values of $[^{18}\text{F}]\mathbf{1}$ were determined by measuring the distribution of this radioligand between *n*-octanol and differently buffered aqueous solutions. As shown in Table 4, experimental log D values determined by the classical shake-flask method were comparable to the theoretical/computed values or slightly lower. As expected, the lipophilicity of the radioligands increased gradually with the length of the fluoroalkyl chain in position 3. Among this series of radiotracers, $[^{18}\text{F}]\mathbf{1}$ has the lowest log D value. However, the log D value of $[^{18}\text{F}]\mathbf{1}$ is still in a promising range allowing the penetration of $[^{18}\text{F}]\mathbf{1}$ into the brain during in vivo experiments.

2.6. In vivo stability in the brain

For the analysis of radiometabolites in the brain of CD-1 mice, $[^{18}\text{F}]\mathbf{1}$ was administered intravenously via the tail vein. At 30 and 60 min post injection (p.i.), brain samples were processed and two-fold extracted with ice-cold acetonitrile. The amount (in %) of parent radiotracer $[^{18}\text{F}]\mathbf{1}$ and radiometabolites in the isolated extracts

after concentration were analyzed by analytical radio-HPLC and -TLC. Generally, good agreement was achieved between these two analytical methods. The recoveries of radioactivity from the brain homogenates in acetonitrile extracts were moderate (75–80% at 30 min p.i. and 60–68% at 60 min p.i.).

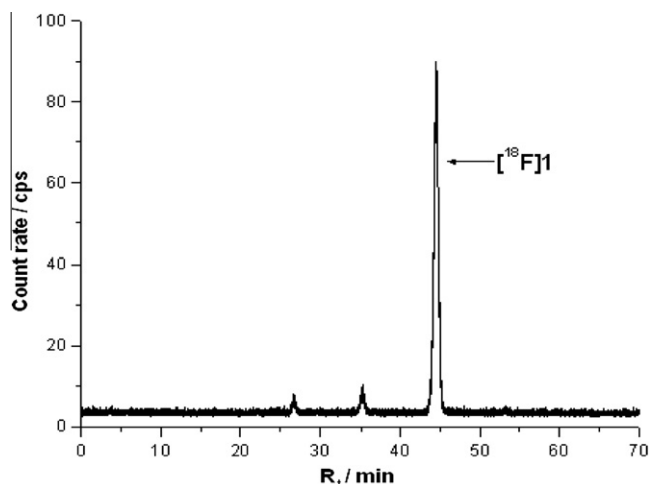


Figure 5. Analytical RP-HPLC chromatogram of the acetonitrile extracts of brain homogenates of CD-1 mice at 30 min p.i. of $[^{18}\text{F}]\mathbf{1}$ (Multospher 120 RP-18 AQ column, 250 × 4.6, 5 μm, 5% MeCN in 20 mM $\text{NH}_4\text{OAc}_{\text{aq}}$ over 50 min, 1 mL/min, $\lambda = 254$ nm).

Table 5

Amount of nonmetabolized radiotracers (in %) in the acetonitrile extracts of brain homogenates at 30 and 60 min p.i. of [^{18}F]1–4 in female CD-1 mice ($n = 3$)

	[^{18}F]1	[^{18}F]2	[^{18}F]3	[^{18}F]4
30 min p.i.	90 ± 1.5	97 ± 1.2	96 ± 1.5	96 ± 1.0
60 min p.i.	79 ± 1.0	98 ± 0.5	98 ± 1.4	95 ± 2.7

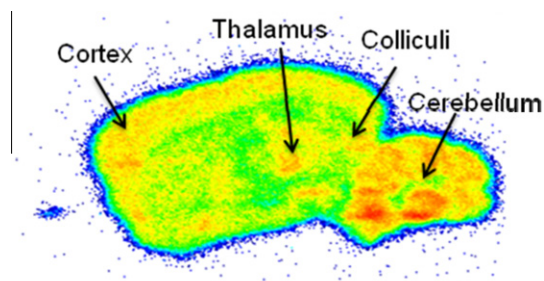


Figure 6. Ex vivo autoradiographs of a sagittal slice of female CD-1 mouse brain at 45 min after i.v. injection of [^{18}F]1 (24 MBq).

At 30 min p.i., 90% of the radioactivity in the brain extracts corresponded to the nonmetabolized radiotracer [^{18}F]1 (Fig. 5, $t_R = 44.4$ min). However, two radiometabolites were also detected ($t_R = 26.7$ min, 4% and $t_R = 35.2$ min, 6%). At 60 min p.i., nonmetabolized [^{18}F]1 and the same radiometabolites were found with 79%, 10%, and 11%, respectively.

This observation is in strong contrast to the in vivo metabolism of the three radiotracers [^{18}F]2–4 previously investigated,^{44–46} where even at 60 min p.i., radiometabolites were not detected and the amount of unchanged radioligand in the brain supernatants always exceeded 95% of total brain radioactivity (Table 5). The current data indicate a slightly lower stability in vivo of the fluoromethyl derivative [^{18}F]1.

Table 6

Distribution of radioactivity in mice after i.v. injection of [^{18}F]1 (300 kBq)

Organ	Radioactivity uptake (% ID/g wet weight) ^a			
	5 min p.i.	30 min p.i.	60 min p.i.	120 min p.i.
Blood	0.73 ± 0.10	0.35 ± 0.05	0.16 ± 0.05	0.15 ± 0.14
Plasma	1.10 ± 0.17	0.55 ± 0.10	0.28 ± 0.21	0.22 ± 0.24
Brain	7.15 ± 1.36	4.56 ± 0.35	2.99 ± 0.73	2.70 ± 0.85
Cerebellum	8.20 ± 2.10	6.27 ± 0.63	4.27 ± 1.23	4.02 ± 0.56
Heart	7.33 ± 2.59	4.57 ± 0.60	2.96 ± 0.53	3.05 ± 0.47
Lung	18.01 ± 3.46	8.30 ± 0.40	8.32 ± 1.71	6.82 ± 2.12
Stomach	2.62 ± 0.19	3.52 ± 0.76	1.77 ± 0.15	1.90 ± 0.27
Small intestine	19.78 ± 2.97	18.82 ± 5.12	23.46 ± 13.39	25.90 ± 12.74
Large intestine	0.91 ± 0.18	1.28 ± 0.47	0.92 ± 0.29	1.46 ± 0.08
Content of intestine	0.39 ± 0.10	0.40 ± 0.05	0.32 ± 0.15	1.96 ± 0.98
Liver	5.31 ± 0.65	6.68 ± 1.37	3.98 ± 0.92	3.95 ± 0.32
Kidney	14.93 ± 4.69	9.61 ± 1.71	6.03 ± 1.20	5.60 ± 0.97
Urine	3.99 ± 2.19	46.35 ± 32.97	45.50 ± 60.25	56.46 ± 12.34
Bladder	1.51 ± 0.40	3.86 ± 0.78	1.42 ± 1.47	5.58 ± 2.99
Spleen	6.23 ± 1.06	8.85 ± 0.76	5.30 ± 0.40	4.84 ± 1.51
Thymus	3.61 ± 1.30	4.83 ± 1.06	2.50 ± 1.00	2.52 ± 0.28
Pancreas	11.22 ± 2.15	16.03 ± 1.37	9.27 ± 3.01	11.99 ± 1.12
Adrenals	13.29 ± 1.13	13.39 ± 0.88	7.48 ± 4.29	6.60 ± 2.43
Gonads	3.26 ± 1.48	4.75 ± 0.96	3.28 ± 1.00	3.55 ± 1.75
Muscle	2.12 ± 0.40	1.67 ± 0.26	0.97 ± 0.37	1.16 ± 0.04
Femur	2.32 ± 1.01	4.34 ± 1.57	1.75 ± 1.13	1.92 ± 0.84
Femur (flushed)	2.09 ± 0.47	1.42 ± 0.68	1.18 ± 0.65	1.29 ± 0.48
Eye	1.89 ± 0.47	2.00 ± 0.34	0.87 ± 0.73	1.53 ± 0.23
Fat	1.12 ± 0.31	1.82 ± 0.38	2.02 ± 0.63	2.08 ± 0.51

^a Mean ± SD ($n = 3$).

2.7. Ex vivo autoradiography

In order to determine the regional distribution of [^{18}F]1, an ex vivo autoradiography of slices of CD-1 mouse brain were performed. At 45 min after i.v. injection of [^{18}F]1, localization of the radioligand correlated with σ_1 receptor-rich regions such as the area of the facial nucleus, the dorsolateral and lateral periaqueductal gray, the dorsomedial hypothalamic area, and the cerebellum (Fig. 6). Moderate radiotracer accumulation was observed in thalamic nuclei and the striatum and the lowest concentration of [^{18}F]1 was detected in the anterior part of the olfactory bulb. Thus, the latter region was chosen as nontarget tissue region. Analyses of the images provided moderate target-to-nontarget tissue ratios for [^{18}F]1 such as, for example, 1.34 for the facial nucleus. This value is the lowest compared to those obtained for the derivatives [^{18}F]2–4 (4.69, 1.97, and 2.83, respectively)^{44–46} at 45 min p.i.

2.8. Organ distribution in CD-1 mice

Table 6 summarizes the data obtained in biodistribution studies in female CD-1 mice at 5, 30, 60, and 120 min after i.v. injection of [^{18}F]1. Results are presented as percentage of the injected dose per gram of wet tissue (% ID/g) for all organs of interest. Interestingly, a high uptake in the brain was observed at 5 min p.i. ($7.15 \pm 1.36\%$ ID/g) but also in σ_1 receptor expressing organs. During the course of the study, the level of radioactivity detected in these tissues decreased continuously.

Generally, organ distribution of [^{18}F]1 and its fluoroalkyl analogs [^{18}F]2–4^{44–46} were comparable for most organs. High radioactivity uptake in the bladder and urine pointed to renal elimination as the major excretory pathway of all four radiotracers. The continuous gastrointestinal accumulation of radioactivity was consistent with an additional hepatobiliary elimination pattern.

Initially, defluorination of [^{18}F]3 was hypothesized, which was the first radiotracer characterized in this series.⁴⁵ As illustrated in Figure 7A, an increased uptake of radioactivity in the femur over time was observed for all radiotracers [^{18}F]2–4^{44–46} except the fluoromethyl derivative [^{18}F]1 with a direct correlation between

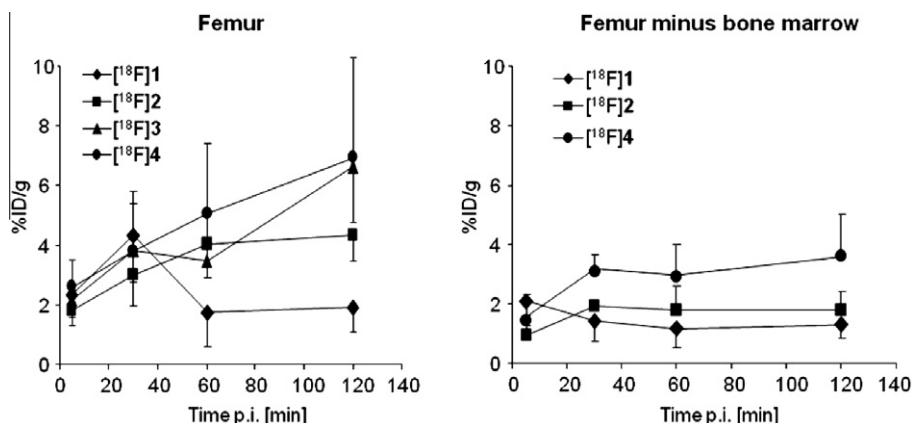


Figure 7. [^{18}F]1–4 uptake in femur and bone marrow of CD-1 mice. Evidence for lack of defluorination. Values are means \pm SD (% ID/g).

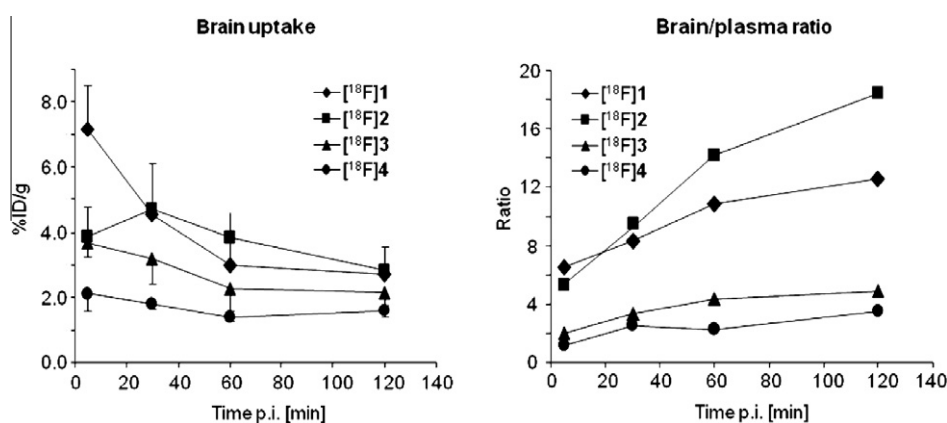


Figure 8. Brain uptake in CD-1 mice and comparison of the brain-to-plasma ratios for [^{18}F]1–4. Values are means \pm SD (% ID/g).

lipophilicity and amount of uptake at 120 min p.i. Therefore, the highly lipophilic bone marrow was isolated from the femur during the biodistribution studies of [^{18}F]2 and [^{18}F]4, and accumulation of radioactivity in this tissue was identified as the reason for the observed increase in femur uptake. The initially assumed defluorination of [^{18}F]3 can be excluded (Fig. 7B). In the present study the uptake of radioactivity in the flushed femur was nearly constant over time and lend support to limited or no defluorination of [^{18}F]1.

As expected, the time-activity data on brain permeation of [^{18}F]1–4 clearly showed that the early brain uptake (5 min p.i.) is inversely related to the lipophilicity of the radiotracers (Fig. 8A). However, at 30 min p.i. only [^{18}F]2 showed an increased brain uptake compared to 5 min p.i. This result indicates specific accumulation of this radiotracer which is most likely related to its highest target affinity within the series under investigation. Accordingly, the brain-to-plasma ratio was considerably higher for [^{18}F]2 than for the other three ^{18}F -labeled spirocyclic piperidine derivatives (Fig. 8B).

3. Conclusion

Herein are described the synthesis and biological characterization of the fluoromethyl derivative **1** which represents the shortest homolog of fluoroalkyl substituted spirocyclic σ ligands **1**–**4**. The fluoromethyl derivative **1** showed very high σ_1 affinity ($K_i = 0.74$ nM) and selectivity against several other related targets. Due to the branched β -position, an efficient radiosynthesis of [^{18}F]1 was only possible upon heating in DMSO at 150 $^\circ\text{C}$ the tosylate **15** in the presence of the $\text{K}[^{18}\text{F}]\text{F}-\text{K}_{222}$ -carbonate complex. Compared with the fluoroalkyl homologs **2**–**4**, the in vitro biotransformation

of **1** with rat liver microsomes was very fast. Moreover, in vivo two radiometabolites of [^{18}F]1 were detected in the mouse brain. This observation is in sharp contrast to the findings obtained with the radiotracers [^{18}F]2–**4**, which do not form radiometabolites in the brain. Whereas [^{18}F]1 provided the lowest target-to-nontarget ratio in ex vivo brain autoradiography experiments, the highest ratio was found for the fluoroethyl derivative [^{18}F]2. Although the early brain uptake (5 min after injection) was inversely related to the lipophilicity of the four homologous radiotracers [^{18}F]1–**4**, the fluoroethyl radiotracer [^{18}F]2 showed the highest accumulation in the brain uptake over a longer period of time, which is presumably due to its very high σ_1 receptor affinity. The good penetration of [^{18}F]1 into the central nervous system is also reflected by the high brain/plasma ratio, which is only exceeded by the fluoroethyl derivative [^{18}F]2. However, because of the presence of radiometabolites in the brain the fluoromethyl derivative **1** is not suitable for neuroimaging of σ_1 receptors. The fluoroethyl derivative **2** has the best properties among the homologous radiotracers [^{18}F]1–**4** and, therefore, will be further developed for clinical studies.

4. Experimental

4.1. Chemistry

4.1.1. General

Unless otherwise noted, moisture sensitive reactions were conducted under dry nitrogen. THF was dried with sodium/benzophenone and was freshly distilled before use. Thin layer chromatography (tlc): silica gel 60 F_{254} plates (Merck). Flash

chromatography (fc): silica gel 60, 40–64 μm (Merck); parentheses include: diameter of the column, eluent, fraction size, R_f value. Melting point: Melting point apparatus SMP 3 (Stuart Scientific), uncorrected. MS: MAT GCQ (Thermo-Finnigan); EI = electron impact; Thermo Finnigan LCQ[®] ion trap mass spectrometer with an electrospray ionization (ESI) interface. IR: IR spectrophotometer 480Plus FT-ATR-IR (Jasco). ¹H NMR (400 MHz), ¹³C NMR (100 MHz): Mercury-400BB spectrometer (Varian); δ in ppm related to tetramethylsilane; coupling constants are given with 0.5 Hz resolution. HPLC: Merck Hitachi Equipment; UV detector: L-7400; autosampler: L-7200; pump: L-7100; degasser: L-7614; Method 1: column: LiChrospher[®] 60 RP-select B (5 μm), 250–4 mm; flow rate: 1.00 mL/min; injection volume: 5.0 μL ; detection at $\lambda = 210$ nm; solvents: A: water with 0.05% (v/v) trifluoroacetic acid; B: acetonitrile with 0.05% (v/v) trifluoroacetic acid; gradient elution: (A%): 0–4 min: 90%, 4 min: 90%, 4–29 min: gradient from 90% to 0%, 29–31 min: 0%, 31–31.5 min: gradient from 0% to 90%, 31.5–40 min: 90%. The purity of all test compounds was greater than 95%, which was determined by the given HPLC method.

4.1.2. 1'-Benzyl-3H-spiro[[2]benzofuran-1,4'-piperidine]-3-carbonitrile (6)³⁸

Under N₂ compound **5** (504 mg, 1.64 mmol) was dissolved in CH₂Cl₂ (17 mL) and the solution was cooled to –25 °C. Then, Me₃SiCN (1.22 mL, 9.7 mmol) and BF₃·Et₂O (0.25 mL, 1.94 mmol) were added and the mixture was stirred for 20 min at –25 °C and for 1 h at 3–5 °C. Methanol (2 mL) and 2 M NaOH (pH 9–10) were added, the layers were separated and the organic layer was extracted with CH₂Cl₂ (4 \times). The combined organic layers were dried (Na₂SO₄), concentrated in vacuo and the residue was purified by fc (3 cm, cyclohexane/ethyl acetate 7:3, 20 mL, R_f 0.22). Colorless oil, yield 432 mg (87%). C₂₀H₂₀N₂O (304.4). MS (EI): $m/z = 304$ [M], 227 [M–Ph], 213 [M–CH₂Ph], 91 [PhCH₂]. IR: $\tilde{\nu}$ (cm^{–1}) = 2944 (C–H), 1044 (C–O), 754 (C–H, 1,2-disubst. arom.), 699 (C–H, monosubst. arom.). ¹H NMR (CDCl₃): δ (ppm) = 1.71 (ddd, $J = 13.8/5.1/2.6$ Hz, 1H, N(CH₂CH₂)₂), 1.92–2.11 (m, 3H, N(CH₂CH₂)₂), 2.41 (br td, $J = 12.0/2.9$ Hz, 1H, N(CH₂CH₂)₂), 2.50 (td, $J = 11.6/3.7$ Hz, 1H, N(CH₂CH₂)₂), 2.82–2.89 (m, 2H, N(CH₂CH₂)₂), 3.59 (s, 2H, NCH₂Ph), 5.86 (s, 1H, ArCHO), 7.19–7.21 (m, 1H, arom. H), 7.25–7.44 (m, 8H, arom. H). ¹³C NMR (CDCl₃): δ (ppm) = 37.1 (1C, N(CH₂CH₂)₂), 37.5 (1C, N(CH₂CH₂)₂), 49.9 (1C, N(CH₂CH₂)₂), 50.1 (1C, N(CH₂CH₂)₂), 63.6 (1C, NCH₂Ph), 69.1 (1C, ArCHCN), 88.3 (1C, ArCO), 118.7 (1C, CN), 121.6 (1C, arom. CH), 122.2 (1C, arom. CH), 127.3 (1C, arom. CH), 128.5 (1C, arom. CH), 129.0 (1C, arom. CH), 129.5 (1C, arom. CH), 130.0 (1C, arom. CH), 134.0 (1C, arom. C), 138.6 (1C, arom. C), 145.7 (1C, arom. C). Purity (HPLC): 99.6%, $t_R = 16.48$ min.

4.1.3. Ethyl 1'-benzyl-3H-spiro[[2]benzofuran-1,4'-piperidine]-3-carboxylate (7)³⁸

The nitrile **6** (211 mg, 0.69 mmol) was dissolved in EtOH. H₂SO₄ concd. (~1.0 g) and three drops of H₂O were added slowly. The mixture was heated to reflux for 19 h. Then 2 M NaOH was added under cooling with ice (pH 8–9). After addition of a saturated solution of NaCl the layers were separated, and the aqueous layer was extracted with CH₂Cl₂ (4 \times). The combined organic layers were dried (Na₂SO₄), the solvent was removed in vacuo and the residue was purified by fc (2 cm, cyclohexane/ethyl acetate 7:3, 10 mL, R_f (cyclohexane/ethyl acetate 5:5) 0.43). Pale yellow oil, yield 138.4 mg (57%). C₂₂H₂₅N₂O₃ (351.4). MS (EI): $m/z = 351$ [M], 260 [M–CH₂Ph], 91 [PhCH₂]. IR: $\tilde{\nu}$ (cm^{–1}) = 2943 (C–H), 1755, (C=O), 1075 (C–O), 755 (C–H, 1,2-disubst. arom.), 700 (C–H, monosubst. arom.). ¹H NMR (CDCl₃): δ (ppm) = 1.28 (t, $J = 7.1$ Hz, 3H, OCH₂CH₃), 1.73 (ddd, $J = 13.5/5.0/2.6$ Hz, 1H, N(CH₂CH₂)₂), 1.93–2.18 (m, 3H, N(CH₂CH₂)₂), 2.48 (td, $J = 12.3/2.7$ Hz, 1H, N(CH₂CH₂)₂), 2.58 (td, $J = 11.3/2.7$ Hz, 1H, N(CH₂CH₂)₂), 2.82–2.90 (m, 2H, N(CH₂CH₂)₂), 3.59 (s, 2H, NCH₂Ph), 4.20 (q, $J = 7.1$ Hz, 2H, OCH₂CH₃), 5.66 (s,

1H, ArCHO), 7.14–7.16 (br d, $J = 8.0$ Hz, 1H, arom. H), 7.23–7.40 (m, 8H, arom. H). Purity (HPLC): 95.6%, $t_R = 17.72$ min.

4.1.4. (1'-Benzyl-3H-spiro[[2]benzofuran-1,4'-piperidin]-3-yl)methanol (8)³⁸

Under N₂ the ester **7** (127 mg, 0.36 mmol) was dissolved in THF (6 mL) and the solution was cooled down to –20 °C. A solution of LiAlH₄ (1 M in THF, 0.74 mL, 0.74 mmol) was added slowly and the mixture was stirred for 30 min at –20 °C. After addition of a saturated solution of NaCl, it was filtered and the filtrate was extracted with CH₂Cl₂ (3 \times). The organic layer was dried (Na₂SO₄), concentrated in vacuo and the residue was purified by fc (2 cm, cyclohexane/ethyl acetate 5:5, 10 mL, R_f 0.17). Colorless oil, yield 80.5 mg (72%). C₂₀H₂₃N₂O₂ (309.4). MS (EI): $m/z = 309$ [M], 218 [M–CH₂Ph], 91 [PhCH₂]. IR: $\tilde{\nu}$ (cm^{–1}) = 3386 (w, O–H), 2917 (C–H), 1050 (C–O), 754 (C–H, 1,2-disubst. arom.), 699 (C–H, monosubst. arom.). ¹H NMR (CDCl₃): δ (ppm) = 1.73 (ddd, $J = 13.8/5.3/2.7$ Hz, 2H, N(CH₂CH₂)₂), 1.96 (td, $J = 13.0/4.4$ Hz, 1H, N(CH₂CH₂)₂), 2.16 (td, $J = 13.2/4.2$ Hz, 1H, N(CH₂CH₂)₂), 2.49 (br t, $J = 11.9$ Hz, 2H, N(CH₂CH₂)₂), 2.82–2.90 (m, 2H, N(CH₂CH₂)₂), 3.61 (s, 2H, NCH₂Ph), 3.75 (dd, $J = 11.6/5.5$ Hz, 1H, CH₂OH), 3.94 (dd, $J = 11.6/3.3$ Hz, 1H, CH₂OH), 5.29 (br t, $J = 4.4$ Hz, 1H, ArCHO), 7.15–7.18 (m, 2H, arom. H), 7.26–7.38 (m, 7H, arom. H). A signal for the OH-proton is not seen in the spectrum. Purity (HPLC): 95.6%, $t_R = 13.28$ min.

4.1.5. 1'-Benzyl-3-(fluoromethyl)-3H-spiro[[2]benzofuran-1,4'-piperidine] (1, WMS-1850)

Under N₂ CH₂Cl₂ (10 mL) was cooled to –78 °C. Then, diethylaminosulfur trifluoride (DAST, 0.2 mL, 1.62 mmol) and 5 min later a solution of alcohol **8** (224.7 mg, 0.73 mmol) in CH₂Cl₂ (5 mL) were added slowly. After stirring for 30 min at –78 °C the mixture was warmed to rt and stirred for 19 h. Then an additional amount of DAST (30 μL , 0.2 mmol) was added at –40 °C and the mixture was stirred for 5 h at rt. Under cooling with ice 2 M NaOH was added (pH >10). The layers were separated and the aqueous layer was extracted with CH₂Cl₂ (4 \times). The combined organic layers were dried (Na₂SO₄), the solvent was removed in vacuo and the residue was purified by fc (2 cm, cyclohexane/ethyl acetate 7:3, 10 mL, R_f (cyclohexane/ethyl acetate 5:5) 0.40). Pale yellow oil, yield 158.7 mg (70%). C₂₀H₂₂FNO₂ (311.4). MS (EI): $m/z = 311$ [M], 234 [M–Ph], 220 [M–CH₂Ph], 91 [PhCH₂]. IR: $\tilde{\nu}$ (cm^{–1}) = 2941 (C–H), 1604 (arom. C=C), 1052 (C–O), 756 (C–H, 1,2-disubst. arom.), 740, 698 (C–H, monosubst. arom.). ¹H NMR (CDCl₃): δ (ppm) = 1.73 (ddd, $J = 13.8/5.6/2.8$ Hz, 2H, N(CH₂CH₂)₂), 1.98 (td, $J = 12.7/3.5$ Hz, 1H, N(CH₂CH₂)₂), 2.07 (td, $J = 12.8/3.9$ Hz, 1H, N(CH₂CH₂)₂), 2.47 (br t, $J = 10.9$ Hz, 1H, N(CH₂CH₂)₂), 2.49 (br t, $J = 10.9$ Hz, 1H, N(CH₂CH₂)₂), 2.84 (br d, $J = 11.1$ Hz, 2H, N(CH₂CH₂)₂), 3.59 (s, 2H, NCH₂Ph), 4.56 (ddd, $J = 47.3/9.7/4.9$ Hz, 1H, CHCH₂F), 4.61 (ddd, $J = 47.3/9.7/3.9$ Hz, 1H, CHCH₂F), 5.40 (dt, $J = 20.4/4.2$ Hz, 1H, ArCHO), 7.16 (br d, $J = 7.2$ Hz, 1H, arom. H), 7.22 (br d, $J = 6.7$ Hz, 1H, arom. H), 7.25–7.38 (m, 7H, arom. H). ¹³C NMR (CDCl₃): δ (ppm) = 37.7 (1C, N(CH₂CH₂)₂), 38.4 (1C, N(CH₂CH₂)₂), 50.1 (1C, N(CH₂CH₂)₂), 50.2 (1C, N(CH₂CH₂)₂), 63.5 (1C, NCH₂Ph), 80.4 (d, $J = 21.1$ Hz, 1C, CHCH₂F), 85.2 (1C, ArCO), 85.4 (d, $J = 174.9$ Hz, 1C, CHCH₂F), 121.3 (1C, arom. CH), 121.8 (1C, arom. CH), 127.2 (1C, arom. CH), 128.0 (1C, arom. CH), 128.4 (2C, arom. CH), 128.5 (1C, arom. CH), 129.5 (2C, arom. CH), 137.1 (d, $J = 5.9$ Hz, 1C, arom. C), 138.5 (1C, arom. C), 146.6 (1C, arom. C). Purity (HPLC): 98.3%, $t_R = 17.35$ min. Elemental analysis: calcd: C, 77.14; H, 7.12; N, 4.50; found: C, 76.55; H, 7.07; N, 4.34.

4.1.6. 3-(Fluoromethyl)-3H-spiro[[2]benzofuran-1,4'-piperidine] (9) and 3-methyl-3H-spiro[[2]benzofuran-1,4'-piperidine] (10)

Pd/C (32 mg, 10% (m/m)) and dried ammonium formate (140 mg, 2.2 mmol) were added to a solution of **1** (127.6 mg, 0.41 mmol) in CH₃OH (10 mL). Under N₂ the mixture was heated

to reflux for 3 h. It was filtered over Celite[®], the filtrate was concentrated in vacuo and the residue was purified by fc (0.5 cm, ethyl acetate/MeOH/NH₃ 9:1:0.2, 5 mL, R_f 0.06). Pale yellow oil, yield 83.1 mg (92%). According to the ¹H NMR spectrum and the HPLC analysis, the isolated product contained **9** and **10** in the ratio 69:31. The products were separated only after N-alkylation. **9**: C₁₃H₁₆FNO (221.3); **10**: C₁₃H₁₇NO (203.3). MS (ESI): *m/z* = 222 [MH (**9**)], 204 [MH (**12**)]. IR (**9+10**): $\tilde{\nu}$ (cm⁻¹) = 3298 (N–H), 2940 (C–H), 1604 (arom. C=C), 1072 (C–O), 754 (C–H, 1,2-disubst. arom.). ¹H NMR (CDCl₃): δ (ppm) = 1.50 (d, *J* = 6.4 Hz, 3 × 0.31H, CHCH₃), 1.68–2.04 (m, 4H, N(CH₂CH₂)₂), 3.00–3.17 (m, 4H, N(CH₂CH₂)₂), 4.57 (ddd, *J* = 47.3/9.7/4.9 Hz, 0.69H, CHCH₂F), 4.61 (ddd, *J* = 47.7/9.7/3.8 Hz, 0.69H, CHCH₂F), 5.29 (q, *J* = 6.4 Hz, 0.31H, ArCHO), 5.41 (dt, *J* = 20.3/4.3 Hz, 0.69H, ArCHO), 7.10–7.18 (m, 1H, arom. H), 7.21–7.36 (m, 3H, arom. H). A signal for the NH-proton is not seen in the spectrum. Purity (HPLC): **9**: 66.6%, *t_R* = 12.01 min; **10**: 30.2%, *t_R* = 13.05 min.

4.1.7. 1'-(4-Fluorobenzyl)-3-(fluoromethyl)-3H-spiro[[2]benzofuran-1,4'-piperidine] (**11**) and 1'-(4-fluorobenzyl)-3-methyl-3H-spiro[[2]benzofuran-1,4'-piperidine] (**12**)

A mixture of the secondary amines **9/10** (37.4 mg, 0.17 mmol), 4-fluorobenzyl chloride (26 μ L, 0.22 mmol), K₂CO₃ (0.118 mg, 0.85 mmol) and CH₃CN (5 mL) was heated to reflux for 8 h and subsequently stirred at rt for 15 h. The mixture was filtered over Celite[®], the solvent was removed in vacuo and the residue was purified by fc (0.7 cm, cyclohexane/ethyl acetate 8:2, 5 mL). In addition to the pure samples 24 mg (ca. 27%) of a mixture was isolated.

11 (R_f (cyclohexane/ethyl acetate 5:5) 0.40): colorless oil, yield 19.6 mg (22%). C₂₀H₂₂F₂NO (329.4). MS (EI): *m/z* = 329 [M], 234 [M–PhF], 220 [M–CH₂PhF], 109 [PhCH₂F]. IR: $\tilde{\nu}$ (cm⁻¹) = 2941 (C–H), 1603 (arom. C=C), 1053 (C–O), 828 (C–H, 1,4-disubst. arom.), 755 (C–H, 1,2-disubst. arom.). ¹H NMR (CDCl₃): δ (ppm) = 1.74 (ddd, *J* = 13.9/5.8/2.8 Hz, 2H, N(CH₂CH₂)₂), 1.97 (td, *J* = 13.1/4.5 Hz, 1H, N(CH₂CH₂)₂), 2.06 (td, *J* = 13.1/4.4 Hz, 1H, N(CH₂CH₂)₂), 2.45 (td, *J* = 11.8/2.5 Hz, 1H, N(CH₂CH₂)₂), 2.48 (td, *J* = 11.8/2.5 Hz, 1H, N(CH₂CH₂)₂), 2.81 (br d, *J* = 11.2 Hz, 2H, N(CH₂CH₂)₂), 3.55 (s, 2H, NCH₂Ph), 4.56 (ddd, *J* = 47.3/9.7/4.9 Hz, 1H, CHCH₂F), 4.61 (ddd, *J* = 47.7/9.7/3.8 Hz, 1H, CHCH₂F), 5.40 (dt, *J* = 20.3/4.3 Hz, 1H, ArCHO), 7.01 (t, *J* = 8.7 Hz, 2H, arom. H), 7.16–7.18 (m, 1H, arom. H), 7.21–7.23 (m, 1H, arom. H), 7.28–7.35 (m, 4H, arom. H). Purity (HPLC): 95.1%, *t_R* = 17.74 min.

12 (R_f (cyclohexane/ethyl acetate 5:5) 0.44): colorless oil, yield 8.0 mg (10%). C₂₀H₂₂FNO (311.4). MS (EI): *m/z* = 311 [M], 216 [M–PhF], 202 [M–CH₂PhF], 109 [PhCH₂F]. IR: $\tilde{\nu}$ (cm⁻¹) = 2939 (C–H), 1602 (arom. C=C), 1071 (C–O), 829 (C–H, 1,4-disubst. arom.), 754 (C–H, 1,2-disubst. arom.). ¹H NMR (CDCl₃): δ (ppm) = 1.49 (d, *J* = 6.4 Hz, 3H, CHCH₃), 1.72 (ddd, *J* = 13.8/5.4/2.7 Hz, 2H, N(CH₂CH₂)₂), 1.88 (td, *J* = 13.0/4.0 Hz, 1H, N(CH₂CH₂)₂), 2.10 (td, *J* = 12.9/4.1 Hz, 1H, N(CH₂CH₂)₂), 2.44 (td, *J* = 14.7/2.3 Hz, 1H, N(CH₂CH₂)₂), 2.47 (td, *J* = 14.7/2.3 Hz, 1H, N(CH₂CH₂)₂), 2.76–2.82 (m, 2H, N(CH₂CH₂)₂), 3.55 (s, 2H, NCH₂Ph), 5.28 (q, *J* = 6.3 Hz, 1H, ArCHO), 7.01 (t, *J* = 7.7 Hz, 2H, arom. H), 7.11–7.15 (m, 2H, arom. H), 7.24–7.28 (m, 2H, arom. H), 7.30–7.34 (m, 2H, arom. H). Purity (HPLC): 97.6%, *t_R* = 17.92 min.

4.1.8. 3-(Fluoromethyl)-1'-(1-phenylethyl)-3H-spiro[[2]benzofuran-1,4'-piperidine] (**13**) and 3-methyl-1'-(1-phenylethyl)-3H-spiro[[2]benzofuran-1,4'-piperidine] (**14**)

A mixture of the secondary amines **9/10** (37.4 mg, 0.17 mmol), 1-bromo-1-phenylethane (30 μ L, 0.22 mmol), K₂CO₃ (0.117 mg, 0.85 mmol) and CH₃CN (5 mL) was heated to reflux for 8 h and subsequently stirred at rt for 15 h. The mixture was filtered over Celite[®], the solvent was removed in vacuo and the residue was purified by fc (0.7 cm, cyclohexane/ethyl acetate 7:3+NH₃

(0.01%), 5 mL). In addition to the pure samples 28 mg (ca. 59%) of the mixture was isolated.

13 (R_f (cyclohexane/ethyl acetate 7:3+NH₃ (0.01%)) 0.29): colorless oil, yield 4.2 mg (7.6%). C₂₁H₂₄FNO (325.4). MS (EI): *m/z* = 325 [M], 310 [M–CH₃], 248 [M–Ph], 91 [CH₂Ph]. IR: $\tilde{\nu}$ (cm⁻¹) = 2938 (C–H), 1601 (arom. C=C), 1052 (C–O), 756 (C–H, 1,2-disubst. arom.), 699 (C–H, monosubst. arom.). ¹H NMR (CDCl₃): δ (ppm) = 1.42 (d, *J* = 6.3 Hz, 3H, NCHArCH₃), 1.66 (ddd, *J* = 13.5/4.7/2.5 Hz, 1H, N(CH₂CH₂)₂), 1.78 (ddd, *J* = 13.5/6.0/2.9 Hz, 1H, N(CH₂CH₂)₂), 1.84–2.13 (m, 2H, N(CH₂CH₂)₂), 2.31–2.50 (m, 2H, N(CH₂CH₂)₂), 2.72 (d broad, *J* = 11.3 Hz, 1H, N(CH₂CH₂)₂), 3.04 (d broad, *J* = 9.8 Hz, 1H, N(CH₂CH₂)₂), 3.45–3.52 (m, 1H, NCH(CH₃)Ar), 4.45–4.66 (m, 2H, CHCH₂F), 5.35 (dt, *J* = 20.4/4.7 Hz, 0.5H, ArCHO), 5.36 (dt, *J* = 20.4/4.7 Hz, 0.5H, ArCHO), 7.16–7.38 (m, 9H, arom. H). Purity (HPLC): 95.5%, *t_R* = 17.92 min.

14 (R_f (cyclohexane/ethyl acetate 7:3+NH₃ (0.01%)) 0.37): Colorless oil, yield 5.8 mg (11.2%). C₂₁H₂₅NO (307.4). MS (EI): *m/z* = 307 [M], 292 [M–CH₃], 230 [M–Ph], 202 [M–CH₃CHPh], 91 [CH₂Ph]. IR: $\tilde{\nu}$ (cm⁻¹) = 2969 (C–H), 1601 (arom. C=C), 1071 (C–O), 754 (C–H, 1,2-disubst. arom.), 700 (C–H, monosubst. arom.). ¹H NMR (CDCl₃): δ (ppm) = 1.42 (d, *J* = 6.5 Hz, 3H, NCHArCH₃), 1.46 (t, *J* = 6.3 Hz, 3H, ArCHCH₃), 1.64 (ddd, *J* = 13.5/4.3/2.8 Hz, 1H, N(CH₂CH₂)₂), 1.76 (ddd, *J* = 13.5/4.8/2.8 Hz, 1H, N(CH₂CH₂)₂), 1.72–1.82 (m, 0.5H, N(CH₂CH₂)₂), 1.91 (td, *J* = 13.1/4.6 Hz, 0.5H, N(CH₂CH₂)₂), 2.02 (td, *J* = 13.3/3.9 Hz, 0.5H, N(CH₂CH₂)₂), 2.14 (td, *J* = 12.9/4.3 Hz, 0.5H, N(CH₂CH₂)₂), 2.28–2.50 (m, 2H, N(CH₂CH₂)₂), 2.63–2.72 (m, 1H, N(CH₂CH₂)₂), 2.98–3.08 (m, 1H, N(CH₂CH₂)₂), 3.48 (q, *J* = 6.5 Hz, 1H, NCH(CH₃)Ar), 5.25 (m, 1H, ArCHO), 7.09–7.14 (m, 2H, arom. H), 7.22–7.27 (m, 2H, arom. H), 7.30–7.37 (m, 5H, arom. H). Purity (HPLC): 98.3%, *t_R* = 18.44 min.

4.1.9. [(1'-Benzyl-3H-spiro[[2]benzofuran-1,4'-piperidin]-3-yl)-methyl] tosylate (**15**)

Under N₂ the alcohol **8** (97 mg, 0.31 mmol), 4-(dimethylamino)pyridine (DMAP, 9.7 mg, 0.08 mmol) and NEt₃ (0.2 mL, 1.44 mmol) were dissolved in CH₂Cl₂ (8 mL) and the solution was cooled down to –25 °C. A solution of *p*-toluenesulfonyl chloride (120 mg, 0.63 mmol) in CH₂Cl₂ (2 mL) was added and the mixture was stirred for 30 min at –25 °C and for 21 h at rt. Diluted NaOH was added, the layers were separated and the aqueous layer was extracted with CH₂Cl₂ (4 ×). The combined organic layers were dried (Na₂SO₄), concentrated in vacuo and the residue was purified by fc (1.7 cm, cyclohexane/ethyl acetate 7:3, 10 mL, R_f (cyclohexane/ethyl acetate 5:5) 0.35).

Colorless oil, yield 127.4 mg (88%). C₂₇H₂₉NO₄S (463.6). MS (EI): *m/z* = 463 [M], 372 [M–CH₂Ph], 308 [M–SO₂PhCH₃], 91 [PhCH₂]. IR: $\tilde{\nu}$ (cm⁻¹) = 2925 (C–H), 1598 (arom. C=C), 1361, 1175 (O₂S=O), 813 (C–H, 1,4-disubst. arom.), 756 (C–H, 1,2-disubst. arom.), 740, 698 (C–H, monosubst. arom.). ¹H NMR (CDCl₃): δ (ppm) = 1.56 (ddd, *J* = 13.6/5.2/2.5 Hz, 1H, N(CH₂CH₂)₂), 1.65 (ddd, *J* = 13.4/5.2/2.5 Hz, 1H, N(CH₂CH₂)₂), 1.92 (td, *J* = 12.9/4.5 Hz, 1H, N(CH₂CH₂)₂), 1.98 (td, *J* = 13.1/4.5 Hz, 1H, N(CH₂CH₂)₂), 2.30 (td, *J* = 12.7/2.5 Hz, 1H, N(CH₂CH₂)₂), 2.38 (td, *J* = 12.5/2.7 Hz, 1H, N(CH₂CH₂)₂), 2.42 (s, 3H, ArCH₃), 2.73 (d broad, *J* = 11.2 Hz, 1H, N(CH₂CH₂)₂), 2.79 (d broad, *J* = 11.3 Hz, 1H, N(CH₂CH₂)₂), 3.56 (s, 2H, NCH₂Ph), 4.15 (dd, *J* = 10.1/5.2 Hz, 1H, CH₂OTos), 4.21 (dd, *J* = 10.1/4.5 Hz, 1H, CH₂OTos), 5.35 (t broad, *J* = 4.8 Hz, 1H, ArCHO), 7.12 (br t, *J* = 7.1 Hz, 2H, arom. H), 7.22–7.37 (m, 9H, arom. H), 7.73 (br d, *J* = 8.3 Hz, 2H, arom. H). Purity (HPLC): 99.2%, *t_R* = 19.39 min.

4.2. Receptor binding studies

Membrane preparations and σ_1 and σ_2 assays were performed as described in Ref. 36,38–41 The protein concentration was determined according to the method of Bradford⁵¹ using bovine serum albumin as standard. The σ_1 assay was performed with the

radioligand [^3H]-(+)-pentazocine (22 Ci/mmol; Perkin Elmer). The thawed membrane preparation (about 75 μg of the protein) was incubated with various concentrations of test compounds, 2 nM [^3H]-(+)-pentazocine, and buffer (50 mM TRIS, pH 7.4) in a total volume of 200 μL for 180 min at 37 °C. The incubation was terminated by rapid filtration through the presoaked filtermats by using the cell harvester. After washing each well five times with 300 μL of water, the filtermats were dried at 95 °C. Subsequently, the solid scintillator was put on the filtermat and melted at 95 °C. After 5 min, the solid scintillator was allowed to solidify at rt. The bound radioactivity trapped on the filters was counted in the scintillation analyzer. The nonspecific binding was determined with 10 μM unlabeled (+)-pentazocine. The K_d -value of the radioligand [^3H]-(+)-pentazocine is 2.9 nM.⁵²

4.3. In vitro biotransformation

4.3.1. Preparation of rat liver microsomes

Frozen rat livers from male Wistar rats were thawed in phosphate buffer pH 7.4 with 0.25 M sucrose and 5 mM EDTA, cut into small pieces and homogenized with a Potter (Elvehjem Potter, B. Braun Biotech International). The homogenization was carried out at 4 °C. The resulting suspension was centrifuged at 10,000g for 15 min at 4 °C. Fat was removed by cellulose. The pellet was resuspended in buffer, the mixture was centrifuged again and afterwards both supernatants were combined. This suspension was transferred into an ultracentrifuge for 60 min at 100,000g and 4 °C. The resulting supernatant (cytosol) was discarded, the pellet washed carefully with buffer, resuspended and the centrifugation repeated. Finally the supernatant was removed, the pellet resuspended in a small amount of phosphate buffer pH 7.4 and the microsome suspension was stored at –80 °C. The protein concentration was determined according to the method of Bradford³ using bovine serum albumin as standard.

4.3.2. Incubation of **1** (WMS-1850) with rat liver microsomes

The incubation was carried out in phosphate buffer pH 7.4 at rt in a circular shaker (IKA vibrax VXR) and contained rat liver microsomes (1.5 mg/mL protein), 0.86 mM MgCl_2 and 2.6 mM NADPH/ H^+ . The concentration of **1** was 260 μM in a final volume of 0.9 mL. Usually, the incubation was stopped after 90 min by addition of cold acetonitrile (–20 °C). The samples were stored for 30 min at –20 °C to complete protein precipitation. After thawing, the samples were centrifuged (10,000g). The supernatant was decanted, filtered with a 0.45 μm (pore size) syringe filter made from regenerated cellulose and finally analyzed.

4.3.3. Degradation of **1** (WMS-1850) during 90 min

Seven incubations of **1** were carried out in phosphate buffer pH 7.4 at rt in a circular shaker containing rat liver microsomes (1.5 mg/mL protein), 0.86 mM MgCl_2 and 2.6 mM NADPH/ H^+ . The concentration of **1** was 320 μM in a total volume of 0.9 mL. During the first hour every 10 min one incubation was stopped by addition of cold acetonitrile (–20 °C). 200 μL of a praziquantel solution (0.6 mg/mL) were added as internal standard resulting in a final concentration of 220 μM in a total volume of 1.1 mL. After 90 min the last incubation was stopped and analyzed. The calibration was carried out with the same matrix except NADPH/ H^+ . All calibration standards were treated in the same way (90 min on the shaker, protein precipitation with acetonitrile, centrifugation, etc.).

4.3.4. HPLC (ESI)–MS

The HPLC–MS system consisted of a Waters Alliance[®] 2690 separations module, a Waters 2487 dual λ absorbance detector and a Thermo Finnigan LCQ[®] ion trap mass spectrometer with an electro

spray (ESI) interface. The ion spray voltage was 3 kV in positive mode at a sheath gas flow of 80 arbitrary units. Temperature of the capillary was set to 200 °C and the capillary voltage to 4 V. A 20 μL volume of the prepared incubation solution was injected onto a LiChrospher[®] RP Select B 5 μm (250 \times 4 mm) column (Merck, Germany) at a flow rate of 1.0 mL/min. The mobile phase was composed of (A) 15% acetonitrile in water and (B) 60% acetonitrile in water. 0.05% trifluoroacetic acid was added to both components. The following gradient was applied (A%): 0 min: 100%, 20 min: 0%, 23 min: 0%, 24 min: 100%, and 30 min: 100%.

In addition to the MS spectra the UV absorption at 210 nm was recorded.

4.4. Radiochemistry

4.4.1. General

No-carrier-added [^{18}F]fluoride (half-life: 109.8 minutes) was produced via the [^{18}O (p, n) ^{18}F] nuclear reaction by irradiation of a [^{18}O]water target (>97%-enriched, 2 mL) on an General Electric PETtrace cyclotron (16.5 MeV proton beam). All radiotracers were shown by radio-TLC or analytical radio-HPLC to be identical to the authentic nonradioactive material and to be free of significant chemical and radiochemical impurities.

4.4.2. [^{18}F]1'-Benzyl-3-(fluoromethyl)-3H-spiro[[2]benzofuran-1,4'-piperidine] ([^{18}F]1)

The aqueous [^{18}F]fluoride solution was azeotropically dried using acetonitrile in the presence of potassium carbonate (1.8 mg) and K_{222} (Kryptofix, 11.2 mg) for [^{18}F]fluoride activation. No-carrier-added aliphatic nucleophilic substitution was performed by reacting tosylate **15** (2.5 mg) in anhydrous DMSO (1 mL) with the dried $\text{K}^{[18}\text{F}]\text{F-K}_{222}$ -carbonate complex at 150 °C under stirring for 20 min. After cooling to room temperature, the labeling efficiencies obtained were controlled by radio-TLC analysis (between 67% and 86%, $n = 4$, SiO_2 , ethyl acetate/petroleum ether/ammonia, 5/5/0.1, v/v/v, $R_f = 0.74$). The crude reaction mixture was diluted with water (3 mL) and directly applied on a semi-preparative radio-HPLC system for purification consisting of a S1021 pump (SYKAM Chromatographie), UV detector (Well-ChromK-2001, KNAUER), NaI(Tl)-counter, data acquisition by an automated system (NINA, Nuclear Interface) on a Multospher 120 RP-18 AQ column with precolumn (150 mm \times 10 mm and 50 mm \times 10 mm, respectively, particle size 5 μm , Chromatographie Service) using the following conditions: isocratic elution, 55% acetonitrile in aqueous 20 mM ammonium acetate, flow rate = 2 mL \cdot min⁻¹, $\lambda = 254$ nm. The collected fractions ([^{18}F]1, $t_R = 37.4$ min) were combined, diluted with water (40–45 mL), passed through a Sep-Pak[®] Plus C-18 cartridge (Waters Corporation), and washed with water (2 \times 5 mL). The radiotracer [^{18}F]1 was eluted using methanol (2 mL). The solvent was carefully evaporated under argon and [^{18}F]1 was dissolved in 0.9% sodium chloride isotonic solution containing 5% of ethanol. Radiochemical yields were obtained between 38 and 50% ($n = 3$). Radio-TLC and analytic radio-HPLC analyses (Multospher 120 RP-18 AQ column, 250 mm \times 4.6 mm, particle size 5 μm , Chromatographie Service, 5% MeCN in aqueous 20 mM ammonium acetate for 5 min and gradient to 80% MeCN in aqueous 20 mM ammonium acetate over 50 min, flow rate = 1 mL \cdot min⁻¹, $\lambda = 254$ nm) revealed a radiochemical purity of 99.4 \pm 0.3% ($n = 6$) and a specific activity usually higher than 375 GBq/ μmol .

4.5. In vitro stability of [^{18}F]1

The radiotracer [^{18}F]1 was incubated at 40 °C for 120 minutes in either 0.9% sodium chloride solution, phosphate-saline-solution (0.1 M sodium phosphate, 0.15 M sodium chloride, pH 7.2) or

0.01 M TRIS–HCl (pH 7.4 at 21 °C). Aliquots were taken from the crude mixtures at selected times points during the experiments and analyzed by radio-TLC (SiO₂, ethyl acetate/petroleum ether/ammonia, 5/5/0.1, v/v/v) and gradient analytical radio-HPLC (Multospher 120 RP-18 AQ column, 250 mm × 4.6 mm, particles size 5 μm, Chromatographie Service, 5% MeCN in aqueous 20 mM ammonium acetate for 5 min and gradient to 80% MeCN in aqueous 20 mM ammonium acetate over 50 min, flow rate = 1 mL·min⁻¹, λ = 254 nm).

4.6. Determination of in vivo stability in brain

The radiotracer [¹⁸F]1 (191 MBq) in 200 μL isotonic solution were injected via the tail vein in CD-1 mice. At 30 or 60 min p.i. animals were sacrificed. After isolation, whole brains (n = 2 per time) were homogenized in 1–2 v/w 50 mM TRIS–HCl, pH 7.4 at 4 °C, in a borosilicate glass cylinder by 10 strokes of a PTFE plunger at a speed of 1000⁻¹ using a Potter S Homogenizer (B. Braun, Germany). The homogenates were extracted using ice-cold acetonitrile according a standard protocol.⁴⁶ After concentration, the supernatants were analyzed by gradient analytical radio-HPLC (Multospher 120 RP-18 AQ column, 250 mm × 4.6 mm, particle size 5 μm, Chromatographie Service, 5% MeCN in aqueous 20 mM ammonium acetate for 5 min and gradient to 80% MeCN in aqueous 20 mM ammonium acetate over 50 min, flow rate = 1 mL·min⁻¹, λ = 254 nm) and radio-TLC (SiO₂, ethyl acetate/petroleum ether/ammonia, 5/5/0.1, v/v/v, R_f = 0.74). Spots on radio-TLC plates were analyzed by radioluminescence recording (BAS-1800 II Bioimaging Analyzer, Fuji Film) followed by evaluation with the AIDA 2.31 software (Raystest).

4.7. Ex vivo autoradiography study

The radiotracer [¹⁸F]1 (24 MBq) in 200 μL isotonic solution were injected via the tail vein into conscious female CD-1 mouse. At 45 min p.i., the animal was sacrificed. After removing the brain, the hemispheres were frozen in isopentane (–35 °C). Then, consecutive 12 μm thick sagittal sections were sliced on a cryostat microtome (Microm), thaw-mounted onto microscope slides, dried with a stream of cold air and exposed to ¹⁸F-sensitive storage phosphor screens (Fuji Film). The image plates were analyzed using a BAS-1800II system bioimaging analyzer (Fuji Film). Scan data were visualized and processed by computer assisted microdensitometry (Aida 2.31, Raystest). Brain structures were confirmed by Nissl staining of the exposed sections.

4.8. Organ distribution study

About 300 kBq of [¹⁸F]1 in 200 μL of 0.9% sodium chloride solution containing 5% of ethanol were injected via the tail vein into conscious female CD-1 mice. At 5, 30, 60, and 120 min p.i., 3–6 animals per time points were anesthetized. Blood and urine samples were collected and the animals were euthanized by luxation of the cervical spine. Organs of interest were dissected. All samples were weighed, and radioactivity was measured in a calibrated γ-counter (WallacWIZARD, Perkin-Elmer). The percentage of the injected dose per gram of wet tissue (% ID/g) was calculated by dividing the tissue counts by the initial dose counts and then by the weight of the tissue sample. Data presented correspond to means values with standard deviation (SD).

Acknowledgment

This work was supported by the *Deutsche Forschungsgemeinschaft*, which is gratefully acknowledged.

References

- Martin, W. R.; Eades, C. G.; Thompson, J. A.; Huppler, R. E.; Gilbert, P. E. *J. Pharmacol. Exp. Ther.* **1976**, *197*, 517.
- Hayashi, T.; Su, T. P. *CNS Drugs* **2004**, *18*, 269.
- Hayashi, T.; Su, T. P. *Curr. Neuropharmacol.* **2005**, *3*, 267.
- Kitaichi, K.; Chabot, J. G.; Moebius, F. F.; Flandorfer, A.; Glossmann, H.; Quirion, R. *J. Chem. Neuroanat.* **2000**, *20*, 375.
- Bowen, W. D.; Hellewell, S. B.; McGarry, K. A. *Eur. J. Pharmacol.* **1989**, *163*, 309.
- Quirion, R.; Bowen, W. D.; Itzhak, Y.; Junien, J. L.; Musacchio, J. M.; Rothman, R. B.; Su, T. P.; Tam, S. W.; Taylor, D. P. *Trends Pharmacol. Sci.* **1992**, *13*, 85.
- Kekuda, R.; Prasad, P. D.; Fei, Y. J.; Leibach, F. H.; Ganapathy, V. *Biochem. Biophys. Res. Commun.* **1996**, *229*, 553.
- Fontanilla, D.; Johannessen, M.; Hajipour, A. R.; Cozzi, N. V.; Jackson, M. B.; Ruoho, A. E. *Science* **2009**, *323*, 934.
- Su, T. P.; Hayashi, T.; Maurice, T.; Buch, S.; Ruoho, A. E. *Trends Pharmacol. Sci.* **2010**, *31*, 557.
- de la Puente, B.; Nadal, X.; Portillo-Salido, E.; Sanchez-Arroyos, R.; Ovalle, S.; Palacios, G.; Muro, A.; Romero, L.; Entrena, J. M.; Baeyens, J. M.; Lopez-Garcia, J. A.; Maldonado, R.; Zamanillo, D.; Vela, J. M. *Pain* **2009**, *145*, 294.
- Diaz, J. L.; Zamanillo, D.; Corbera, J.; Baeyens, J. M.; Maldonado, R.; Pericas, M. A.; Vela, J. M.; Torrens, A. *Cent. Nerv. Syst. Agents Med. Chem.* **2009**, *9*, 172.
- Navarro, G.; Moreno, E.; Aymerich, M.; Marcellino, D.; McCormick, P. J.; Mallol, J.; Cortes, A.; Casado, V.; Canela, E. I.; Ortiz, J.; Fuxe, K.; Lluís, C.; Ferré, S.; Franco, R. *Proc. Natl. Acad. Sci. U.S.A.* **2010**, *107*, 18676.
- Hayashi, T.; Su, T. P. *Expert Opin. Ther. Targets* **2008**, *12*, 45.
- Lucas, G.; Rymar, V. V.; Sadikot, A. F.; Debonnel, G. *Int. J. Neuropsychopharmacol.* **2008**, *11*, 485.
- Kishi, T.; Yoshimura, R.; Okochi, T.; Fukuo, Y.; Kitajima, T.; Okumura, T.; Tsunoka, T.; Kawashima, K.; Yamanouchi, Y.; Kinoshita, Y.; Umene-Nakano, W.; Naitoh, H.; Nakamura, J.; Ozaki, N.; Iwata, N. *Neuropharmacology* **2010**, *58*, 1168.
- Sabino, V.; Cottone, P.; Parylak, S. L.; Steardo, L.; Zorrilla, E. P. *Behav. Brain Res.* **2009**, *198*, 472.
- Hindmarch, I.; Hashimoto, K. *Hum. Psychopharmacol.* **2010**, *25*, 193.
- Furuse, T.; Hashimoto, K. *Ann. Gen. Psychiatry* **2009**, *8*, 26.
- Furuse, T.; Hashimoto, K. *Ann. Gen. Psychiatry* **2010**, *9*, 18.
- Hashimoto, K. *CNS Neurol. Disord. Drug Targets* **2009**, *8*, 470.
- Paschos, K. A.; Veletza, S.; Chatzaki, E. *CNS Drugs* **2009**, *23*, 755.
- Kulkarni, S. K.; Dhir, A. *Expert Rev. Neurother.* **2009**, *9*, 1021.
- Maurice, T.; Su, T. P. *Pharmacol. Ther.* **2009**, *124*, 195.
- Fishback, J. A.; Robson, M. J.; Xu, Y. T.; Matsumoto, R. R. *Pharmacol. Ther.* **2010**, *127*, 271.
- Cobos, E. J.; Entrena, J. M.; Nieto, F. R.; Cendan, C. M.; Del Pozo, E. *Curr. Neuropharmacol.* **2008**, *6*, 344.
- Toyohara, J.; Sakata, M.; Ishiwata, K. *Cent. Nerv. Syst. Agents Med. Chem.* **2009**, *9*, 190.
- Mishina, M.; Ishiwata, K.; Ishii, K.; Kitamura, S.; Kimura, Y.; Kawamura, K.; Oda, K.; Sasaki, T.; Sakayori, O.; Hamamoto, M.; Kobayashi, S.; Katayama, Y. *Acta Neurol. Scand.* **2005**, *112*, 103.
- Mishina, M.; Ohya, M.; Ishii, K.; Kitamura, S.; Kimura, Y.; Oda, K.; Kawamura, K.; Sasaki, T.; Kobayashi, S.; Katayama, Y.; Ishiwata, K. *Ann. Nucl. Med.* **2008**, *22*, 151.
- Ishiwata, K.; Ishii, K.; Kimura, Y.; Kawamura, K.; Oda, K.; Sasaki, T.; Sakata, M.; Senda, M. *Ann. Nucl. Med.* **2008**, *22*, 411.
- Sakata, M.; Kimura, Y.; Naganawa, M.; Ishikawa, M.; Oda, K.; Ishii, K.; Hashimoto, K.; Chihara, K.; Ishiwata, K. *Ann. Nucl. Med.* **2008**, *22*, 143.
- Shidahara, M.; Seki, C.; Naganawa, M.; Sakata, M.; Ishikawa, M.; Ito, H.; Kanno, I.; Ishiwata, K.; Kimura, Y. *Ann. Nucl. Med.* **2009**, *23*, 163.
- Matsuno, K.; Nakazawa, M.; Okamoto, K.; Kawashima, Y.; Mita, S. *Eur. J. Pharmacol.* **1996**, *306*, 271.
- Lever, J. R.; Gustafson, J. L.; Xu, R.; Allmon, R. L.; Lever, S. Z. *Synapse* **2006**, *59*, 350.
- Shiba, K.; Ogawa, K.; Ishiwata, K.; Yajima, K.; Mori, H. *Bioorg. Med. Chem.* **2006**, *14*, 2620.
- Berardi, F.; Ferorelli, S.; Colabufo, N. A.; Leopoldo, M.; Perrone, R.; Tortorella, V. *Bioorg. Med. Chem.* **2001**, *9*, 1325.
- Große Maestrup, E.; Wiese, C.; Schepmann, D.; Hiller, A.; Fischer, S.; Scheunemann, M.; Brust, P.; Wünsch, B. *Bioorg. Med. Chem.* **2009**, *17*, 3630.
- Jasper, A.; Schepmann, D.; Lehmkühl, K.; Vela, J. M.; Buschmann, H.; Holenz, J.; Wünsch, B. *Eur. J. Med. Chem.* **2009**, *44*, 4306.
- Maier, C. A.; Wünsch, B. *J. Med. Chem.* **2002**, *45*, 4923.
- Maier, C. A.; Wünsch, B. *J. Med. Chem.* **2002**, *45*, 438.
- Oberdorf, C.; Schepmann, D.; Vela, J. M.; Diaz, J. L.; Holenz, J.; Wünsch, B. *J. Med. Chem.* **2008**, *51*, 6531.
- Schläger, T.; Schepmann, D.; Wurthwein, E. U.; Wünsch, B. *Bioorg. Med. Chem.* **2008**, *16*, 2992.
- Wiese, C.; Große Maestrup, E.; Schepmann, D.; Vela, J. M.; Holenz, J.; Buschmann, H.; Wünsch, B. *J. Pharm. Pharmacol.* **2009**, *61*, 631.
- Wiese, C.; Große Maestrup, E.; Schepmann, D.; Grimme, S.; Humpf, H. U.; Brust, P.; Wünsch, B. *Chirality* **2011**, *23*, 148.
- Fischer, S.; Wiese, C.; Große Maestrup, E.; Hiller, A.; Deuther-Conrad, W.; Scheunemann, M.; Schepmann, D.; Steinbach, J.; Wünsch, B.; Brust, P. *Eur. J. Nucl. Med. Mol. Imaging* **2011**, *38*, 540.

45. Große Mastrup, E.; Fischer, S.; Wiese, C.; Schepmann, D.; Hiller, A.; Deuther-Conrad, W.; Steinbach, J.; Wünsch, B.; Brust, P. *J. Med. Chem.* **2009**, *52*, 6062.
46. Maisonial, A.; Große Mastrup, E.; Fischer, S.; Hiller, A.; Scheunemann, M.; Wiese, C.; Schepmann, D.; Steinbach, J.; Deuther-Conrad, W.; Wünsch, B.; Brust, P. *Chem. Med. Chem.* **2011**, *6*, 1401.
47. Große Mastrup, E.; Wiese, C.; Schepmann, D.; Brust, P.; Wünsch, B. *Bioorg. Med. Chem.* **2011**, *19*, 393.
48. Ram, S.; Spicer, L. D. *Tetrahedron Lett.* **1987**, *28*, 515.
49. Wirt, U.; Schepmann, D.; Wünsch, B. *Eur. J. Org. Chem.* **2007**, 462.
50. Holl, R.; Jung, B.; Schepmann, D.; Humpf, H.-U.; Grünert, R.; Bednarski, P. J.; Englberger, W.; Wünsch, B. *Chem. Med. Chem.* **2009**, *4*, 2111.
51. Bradford, M. M. *Anal. Biochem.* **1976**, *72*, 248.
52. DeHaven-Hudkins, D. L.; Fleissner, L. C.; Ford-Rice, F. Y. *Eur. J. Pharmacol.* **1992**, *722*, 371.